

# A comparison of light path equations in General Relativity using a Taylor series approach vs Jacobian elliptic functions

Gerald Malczewski<sup>1</sup>

## Abstract:

Using a method to calculate the deflection of light near the Sun based on General Relativity (GR), a formula is derived which expresses the light path as a function of the radial distance  $r$  from a gravitating central body. This method, based on the GR geodesic equation applied to the Schwarzschild metric, uses an infinite Taylor series expansion. This requires a 'finite cutoff' of the series to compute the polar angle of a light path coordinate for a given radial distance. We take the light path to be a trajectory of a light ray originating at radial infinity and then departing to radial infinity after reaching its point of closest approach to the central body. Constraints are found that limit the discussion to central bodies of mass  $M$  which obey  $M/R < 1/3$  where  $R$  is the turning point, the point of closet approach.

A comparison is then made with a different approach previously published using Jacobian elliptic functions which yields a closed expression for the light path equation. It is shown that the two approaches are equivalent if a finite cutoff is not taken for the Taylor series. If the cutoff is taken, then computationally the two methods yield approximately the same result for light path locations near the point of closest approach to the central body.

The elliptic function method has the advantage that the method can be applied to the case where  $M/R \geq 1/3$ , including calculating light paths inside a black hole horizon. This case is outside the scope of this paper.

## A. Introduction:

---

<sup>1</sup> Email: MalczewskiGld@gmail.com

The observational validation in 1919 of the value of light deflection by the sun as predicted by Einstein was the first of many validations [4], of the Theory of General Relativity (GR) [2,3,6,9]. In this paper we focus on the light path itself as a function of radial distance from the gravitating body, not the deflection measured by an observer, and compare two different methods derived from GR.

**Sections B and C** derive a light path equation using results from [9] which leverages the GR geodesic equation for the Schwarzschild gravitational metric for a body of with mass  $M$ . The derivation of this light path equation uses a Taylor Series expansion, so a finite cut-off is then required when doing an actual computation. Some examples are given.

**Section D** describes the light path equation derived from Jacobian elliptic functions developed in [5]. Computational examples are also included.

**Section E** compares the models introduced in Sections C and D.

We end with a **Summary** section highlighting the main observations and findings.

The reader is assumed to have basic familiarity with General Relativity, how light reflection is measured (for example, see [8] and section 6.3 of [9]), and some familiarity with impact parameter analysis but detailed knowledge of the mathematical techniques of GR is not required. There is minimal use of tensors and only in the context of the Schwarzschild metric.

As a caution to the reader, the key equations in this paper are drawn from several sources, each with their own notation and conventions. This will necessitate performing multiple sets of notational replacements and transformations which, although adding to the mathematical exposition, will be necessary to demonstrate our assertions. Attempting to show all the derivations for the key equations of each source would result in an excessively long paper and therefore the reader is referred to these sources for the details.

## B. Derivation of light path using Taylor series:

Throughout this paper we assume the gravitating body mass is a perfectly symmetric and static spherical mass with uniform density where rotation and charge are not present or negligible, i.e., the metric is Schwarzschild (see endnote [1] for a description). For most purposes, the body will be treated as a point-like mass with Schwarzschild radius  $\alpha$  so that the light path will not impinge on the body.

We will designate the sought-after light path equation by the function  $\theta = \theta(\rho)$  for a given mass where  $\theta$  is the polar angle of the light path location. The argument  $\rho$  equals  $R/r$  where  $r$  is the radial distance to the center of the body and  $R$  the distance of closet approach.

Conveniently, the preliminary groundwork to find  $\theta(\rho)$  has been done. In Wald [9], planetary orbital precession and light deflection calculations are developed based on the Schwarzschild metric, its space-time geodesics, and impact parameter analysis. As part of the derivations the following equation, in Wald's original notation, is developed for the trajectory of light (see (6.3.41) in his text):

$$\Delta\phi = 2 \int_0^{1/R_0} \frac{du}{\sqrt{R_0^{-2} - 2MR_0^{-3} - u^2 + 2Mu^3}} \quad (1)$$

where  $\Delta\phi$  is the total change in the spherical coordinates polar angle as the light ray propagates in a plane along a path originating at a far distance and terminating at radial distance  $r = R_0$ . See Fig.1. Also  $u \equiv 1/r$  and  $R_0$  is the 'turning point' of the light path which is the point of closest approach to the central body. The constant  $M$  is mass expressed in meters (see endnote [2]). The integration limits represent the end points of the light path;  $u = 0$  ( $r = \infty$ ) is interpreted as the light path originating at a far distance in the direction of some asymptotic line drawn from the origin as shown in Fig. 1. The light paths discussed in this paper all possess asymptotic lines as can be determined by letting  $r \rightarrow \infty$  in the characteristic

equation of the light path. The factor 2 is present since the upper and lower paths are symmetric.

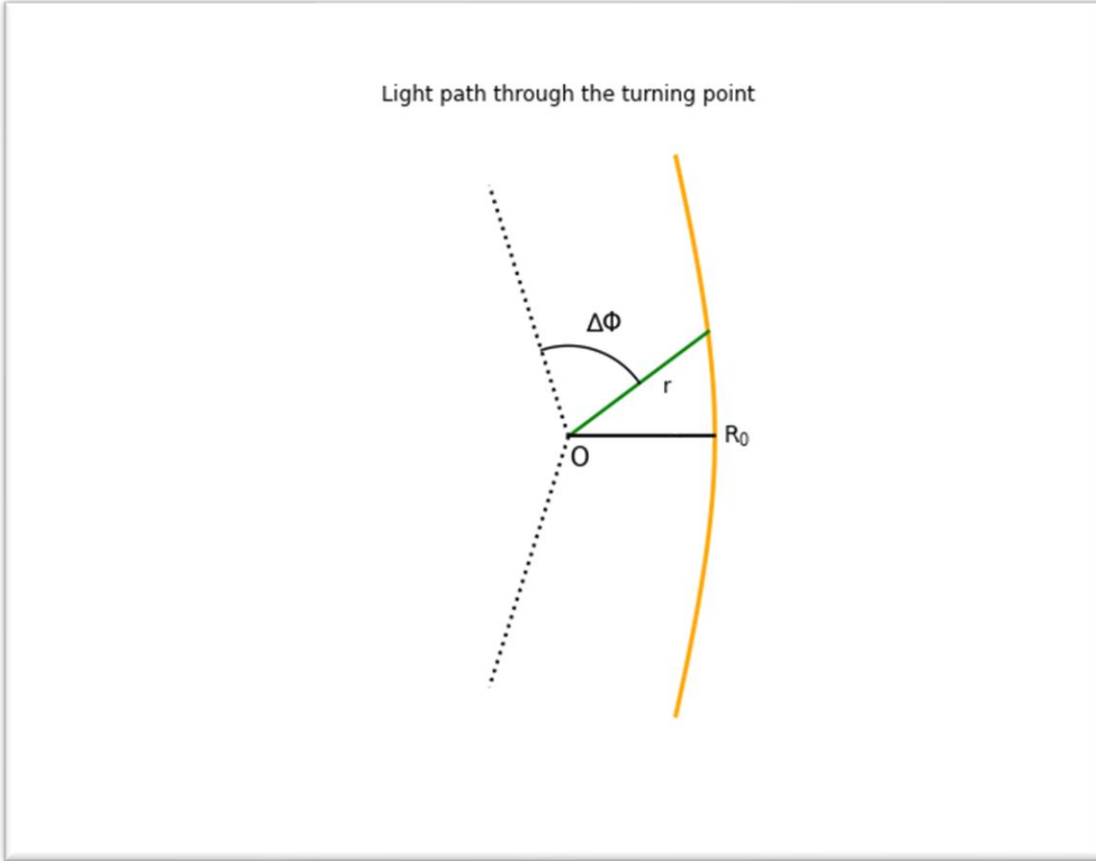


Figure 1. Arbitrary curved light path due to the influence of gravity for a mass at the origin  $O$ , using the notation of Wald [9]. The swept angle  $\Delta\Phi$  and corresponding radial distance  $r$  are shown as the light path moves inbound from a far distance along the asymptote (upper dotted line) through the turning point  $R_0$  and continues outbound asymptotically toward the lower dotted line.

Writing (1) in the differential form, ignoring the factor of 2, and doing the replacement  $\phi \rightarrow \theta$  and  $R_0 \rightarrow R$  to be consistent with the notation we will be using:

$$d\theta = \frac{du}{\sqrt{R^{-2} - 2MR^{-3} - u^2 + 2Mu^3}}, \quad (2)$$

where  $d\theta$  is the infinitesimal polar angle element. Finding the antiderivative by evaluating the integral  $\int d\theta$  with an appropriate change in variables will give us the trajectory function  $\theta(\rho)$  we seek. This is where the mathematical complexity of General Relativity becomes manifest.  $\int d\theta$  is in fact intractable if seeking to express it with elementary functions. We need to express the integrand as a product of two factors where one factor can be expanded as an infinite Taylor series resulting in an infinite sum of tractable integrals. A 'finite cutoff' is then taken to some desired approximation. Going from an intractable form to a series of tractable forms comes at the cost of approximating our desired function  $\theta(\rho)$  for any numerical calculation.

To aid in finding the right factorization we specify some conditions that the antiderivative should have:

#1. When  $M = 0$  (flat space), the light path should be a straight-line trajectory. The equation of a straight line in polar coordinates can be expressed with the sine of  $\theta$  so the antiderivative should equal the  $\sin^{-1}x$  for some  $x$  that should be a function of  $r$  and  $R$ . Then the integral will reduce to the form  $\int \frac{dx}{\sqrt{1-x^2}} = \sin^{-1}x$ .

#2. When  $M = 0$  all other terms in the Taylor series should be suppressed, so  $M$  should be a factor in each series term except the first term  $\sin^{-1}x$  corresponding to the massless case.

#3. The antiderivative should yield  $\theta = \pi/2$  when  $r = R$ , the position of the light path at the turning point.

Now set  $\rho = \frac{R}{r}$ . Then  $0 \leq \rho \leq 1$  and  $\rho = Ru$ . So  $d\rho = Rdu$  or  $du = \frac{1}{R}d\rho$ .

Transforming (2):

$$d\theta = \frac{d\rho}{R\sqrt{R^{-2}-2MR^{-3}-\left(\frac{\rho}{R}\right)^2+2M\left(\frac{\rho}{R}\right)^3}} = \frac{d\rho}{\sqrt{R^2\left[R^{-2}-2MR^{-3}-\left(\frac{\rho}{R}\right)^2+2M\left(\frac{\rho}{R}\right)^3\right]}} = \frac{d\rho}{\sqrt{\left[1-2MR^{-1}-\rho^2+2M\rho^3R^{-1}\right]}} = \frac{d\rho}{\sqrt{\left[1-\rho^2-\frac{2M}{R}(1-\rho^3)\right]}}. \quad (3)$$

We need to ensure that the radicand obeys  $1 - \rho^2 - \frac{2M}{R}(1 - \rho^3) > 0$  or  $\frac{1 - \rho^2}{1 - \rho^3} > \frac{2M}{R}$ . But the LHS of this inequality is in the range  $\frac{2}{3} \leq \frac{1 - \rho^2}{1 - \rho^3} \leq 1$ . If we impose  $\frac{M}{R} < \frac{1}{3}$  then  $\frac{2M}{3} < \frac{1 - \rho^2}{1 - \rho^3} \leq 1$ . Hence  $\frac{1 - \rho^2}{1 - \rho^3} > \frac{2M}{R}$  and positivity is assured.

$\int d\theta$  is still intractable but notice that when  $M = 0$  the expression reduces to  $\frac{d\rho}{\sqrt{1 - \rho^2}}$  which satisfies condition #1. But we need to express (3) as two factors and transform it into a series of terms, each integrable. The presence of the  $\sqrt{1 - \rho^2}$  term suggests the following:

$$\frac{d\rho}{\sqrt{\left[1 - \rho^2 - \frac{2M}{R}(1 - \rho^3)\right]}} \frac{1}{\sqrt{1 - \rho^2}} = \frac{d\rho}{\sqrt{\left[1 - \rho^2 - \frac{2M}{R}(1 - \rho^3)\right]}} \frac{1}{\sqrt{1 - \rho^2}} = \frac{d\rho}{\sqrt{\left[1 - \frac{2M}{R}\left(\frac{1 - \rho^3}{1 - \rho^2}\right)\right]}} \frac{1}{\sqrt{1 - \rho^2}} \quad (4)$$

Then

$$d\theta = \frac{d\rho}{\sqrt{\left[1 - \frac{2M}{R}\left(\frac{1 - \rho^3}{1 - \rho^2}\right)\right]}} \frac{1}{\sqrt{1 - \rho^2}} = \frac{d\rho}{\sqrt{[1 - z]}} \frac{1}{\sqrt{1 - \rho^2}} \quad \text{where } z = \frac{2M}{R} \left(\frac{1 - \rho^3}{1 - \rho^2}\right) \quad (5)$$

which is now in our desired form.

As a check on dimensional consistency note that  $M$ ,  $R$ , and  $r$  all have dimension of length. Therefore,  $\rho$ ,  $M/R$ , and all factors and terms are dimensionless which is required for the polar angle differential  $d\theta$  to be dimensionless.

The restriction on  $M/r < 1/3$  can also be justified using the relationship (see Wald [9], Section 6.3)

$$R_0 = \frac{2b}{\sqrt{3}} \cos\left(\frac{1}{3} \cos^{-1}\left(\frac{-\sqrt{27M}}{b}\right)\right). \quad (6)$$

Here,  $b$  is the impact parameter and  $R_0 = R$ . If  $b$  is larger than the critical value  $\sqrt{27M}$  then the light ray is not captured by

the central body. Using (6) it can be shown that  $M/R < 1/3$  must hold for  $b > \sqrt{27}M$  to be satisfied.

Since  $\frac{2M}{R} < \frac{2}{3}$  and therefore  $\frac{2M}{R} \left( \frac{1-\rho^3}{1-\rho^2} \right) < 1$  we can expand  $\frac{1}{\sqrt{1-Z}}$  as a Taylor series with each term except the first containing a power of  $M$  satisfying condition #2 above:

$$\frac{1}{\sqrt{1-Z}} = 1 + \frac{1}{2}Z + \frac{3}{8}Z^2 + \frac{5}{16}Z^3 + \dots + \frac{(2k-3)!!}{2^{k-1}(k-1)!} Z^{k-1} + \dots \quad (7)$$

for  $k = 1, 2, \dots$ .

Each term of these terms is generated from the formula for a Taylor series, namely  $\sum_1^\infty \frac{f^{[k-1]}(a)}{(k-1)!} (z-a)^{k-1}$ , where  $f^{[k-1]}(a)$  denotes the  $(k-1)$  derivative of the function  $f(z) = [1-z]^{-(1/2)}$ , evaluated at  $a$ , where  $a=0$  is chosen. The details of this calculation are not supplied here, but computing the first few terms of the series should satisfy the reader of its validity.

Then (5) is expressed as

$$d\theta = \left[ \frac{1}{\sqrt{1-\rho^2}} \right] \left[ 1 + \frac{1}{2}Z + \frac{3}{8}Z^2 + \frac{5}{16}Z^3 + \dots + \frac{(2k-3)!!}{2^{k-1}(k-1)!} Z^{k-1} + \dots \right] d\rho. \quad (8)$$

Note the use of the double factorial in the numerator. For  $k=1$  we use the property that  $(-1)!! = 1$ . Integrating and ignoring for the moment the constant of integration

$$\theta = \int \left[ \frac{1}{\sqrt{1-\rho^2}} \right] \left[ 1 + \frac{1}{2}Z + \frac{3}{8}Z^2 + \frac{5}{16}Z^3 + \dots + \frac{(2k-3)!!}{2^{k-1}(k-1)!} Z^{k-1} + \dots \right] d\rho.$$

Each term equals  $\frac{(2k-3)!!}{(2^{k-1})(k-1)!} \left( 2 \left( \frac{1-\rho^3}{1-\rho^2} \right) \frac{M}{R} \right)^{k-1}$  which simplifies to

$\frac{(2k-3)!!}{(k-1)!} \cdot \left( \left( \frac{1-\rho^3}{1-\rho^2} \right) \frac{M}{R} \right)^{k-1}$ . Applying our known bounds gives

$$0 < \frac{(2k-3)!!}{(k-1)!} \left( \left( \frac{1-\rho^3}{1-\rho^2} \right) \frac{M}{R} \right)^{k-1} < \frac{(2k-3)!!}{(k-1)!} \cdot \left( \frac{3}{2} \right)^{k-1} \cdot \left( \frac{1}{3} \right)^{k-1}.$$

Applying the ratio test<sup>2</sup> for infinite series term on the RHS, where we replace the power of 1/3 by  $\frac{1}{3} - \epsilon$  for  $0 < \epsilon \ll 1$ , shows that our infinite series is convergent for any  $M/R < 1/3$  which allows us to distribute  $\int \left[ \frac{1}{\sqrt{1-\rho^2}} \right]$  across each term giving

$$\theta = \int \left[ \frac{1}{\sqrt{1-\rho^2}} + \frac{1}{\sqrt{1-\rho^2}} \left( \frac{(1-\rho^3)M}{(1-\rho^2)R} \right)^1 + \frac{3}{2} \frac{1}{\sqrt{1-\rho^2}} \left( \frac{(1-\rho^3)M}{(1-\rho^2)R} \right)^2 + \frac{5}{2} \frac{1}{\sqrt{1-\rho^2}} \left( \frac{(1-\rho^3)M}{(1-\rho^2)R} \right)^3 + \dots + \frac{(2k-3)!!}{(k-1)!} \frac{1}{\sqrt{1-\rho^2}} \left( \frac{(1-\rho^3)M}{(1-\rho^2)R} \right)^{k-1} + \dots \right] d\rho \quad (9)$$

Then the polar angle function  $\theta = \theta(\rho)$  is just the sum of the antiderivative of each term in the integrand plus the constant of integration.

An alternative derivation of (9) can be conducted starting with equation (3) in Section C.1 of Malczewski and Selig [8],

$$\frac{d\theta}{dr} = \frac{\left[ \frac{1}{r^2} \sqrt{\frac{R^3}{R-2M}} \right]}{\left[ \left( \sqrt{1 - \left( \frac{R}{r} \right)^3 \frac{r-2M}{R-2M}} \right) \right]'}$$

where we have done the notation replacement consistent with our notation in this paper. This demonstration also utilizes the GR geodesic equation applied to the Schwarzschild metric.

N.B. The paper [8], Section C.2, Step E, contains the erroneous general formula  $\frac{2k+1}{2^{2k+1}} z^{k+1}$  for  $k=0,1,2,\dots$  instead of  $\frac{(2k-3)!!}{2^{k-1}(k-1)!} z^{k-1}$  for  $k=1,2,\dots$ . This affects the values of the numeric coefficients beyond the second order terms. However, this does not change the deflection angle calculations in that paper since the infinite series is cut-off, and the second order and higher terms are dropped. A future version of this paper will correct the error.

---

<sup>2</sup> Consult any calculus text

Still another alternative derivation of (9) can be conducted starting with equation (53) in section 13 of Magnan [7] after the necessary notational replacement and algebraic manipulation of differentials.

In all these various methods, the mathematical work is done to determine the deflection angle of the light path. In this paper we will leverage some of that work to instead obtain the equation of the entire trajectory of the path.

Continuing with our main development and using the first two terms of the integrand in (9) we have

$$\int \left( \frac{1}{\sqrt{1-\rho^2}} + \frac{1}{\sqrt{1-\rho^2}} \frac{1-\rho^3}{1-\rho^2} \frac{M}{R} \right) d\rho. \quad (10)$$

Taking antiderivatives.

$$\theta_2(\rho) = \sin^{-1} \rho - \left( \frac{M}{R} \right) \frac{2+\rho}{\sqrt{1+\rho}} \sqrt{1-\rho} + C_2 \quad (11)$$

where the subscript 2 has been inserted and denotes that this result is based on the first two terms of equation (9). When the light ray reaches the point along its path where  $r = R$  its polar angle is  $\pi/2$  in our reference system. This gives us a boundary condition to solve for  $C_2$  which is our condition #3 above. Then  $\theta = \frac{\pi}{2}$  when  $\rho = R/r = 1$ , hence  $\theta_2(1) = \frac{\pi}{2}$ . Then (11) implies

$$C_2 = \frac{\pi}{2} - \sin^{-1} 1 + \left( \frac{M}{R} \right) \frac{2+1}{\sqrt{1+1}} \sqrt{1-1} = 0. \quad (12)$$

Extending this argument to the next level of approximation to include the antiderivative of the third term of (9) we find

$$\theta_3(\rho) = \sin^{-1} \rho - \left( \frac{M}{R} \right) \frac{2+\rho}{\sqrt{1+\rho}} \sqrt{1-\rho} + \frac{3}{2} \left[ \frac{5}{2} \sin^{-1} \rho - \frac{((\sqrt{1-\rho})(3\rho^3+6\rho^2-7\rho-8))}{6(\rho+1)^{3/2}} \right] \left( \frac{M}{R} \right)^2 + C_3. \quad (13)$$

Using the same boundary condition as above to find  $C_3$  we have

$$C_3 = \theta_3(1) - \left\{ \sin^{-1} 1 + \left(\frac{M}{R}\right) \frac{2+1}{\sqrt{1+1}} \sqrt{1-1} + \frac{3}{2} \left[ \frac{5}{2} \sin^{-1} 1 - \frac{((\sqrt{1-1})(3 \cdot 1^3 + 6 \cdot 1^2 - 7 \cdot 1 - 8))}{6(1+1)^{3/2}} \right] \left(\frac{M}{R}\right)^2 \right\} = \pi/2 - \left\{ \pi/2 + 0 + \frac{3}{2} \left[ \frac{5}{2} \cdot \frac{\pi}{2} - 0 \right] \left(\frac{M}{R}\right)^2 \right\} = -\frac{15\pi}{8} \left(\frac{M}{R}\right)^2. \quad (14)$$

Equations (13) and (11) can both be viewed as equations for the GR based light path as a function of  $\rho$ , but to different levels of approximation. The light path constructed from the GR polar angle function  $\theta_n = \theta_n(\rho)$  can also be described in the language of mathematical sets by the infinite set of ordered pairs  $\{(\theta_n(\rho), \rho)\}_\rho$  where  $n$  is the level of approximation and the subscript  $\rho$  ranges over all values between 0 and 1, corresponding to  $r$  ranging over the values  $\infty$  to  $R$ . This set represents the upper half of the entire path. The lower half of the path is symmetric to the upper half with respect to the  $y$ -axis in our spherical coordinate system (using the physics convention).

### C. Predicted polar angle using additional anti-derivatives:

To obtain a better approximation of the predicted polar angle, we now extend the above results to  $\theta_n(\rho)$  for  $n > 3$ . This is done by including additional terms determined by the antiderivatives of the first  $n$  integrand terms in (9). Let the  $k$ th antiderivative, excluding the constant of integration, be denoted by  $F_k(\rho)$ .

An integral calculator shows that the antiderivative for the  $k$ th

term  $\frac{(2k-3)!!}{(k-1)!} \frac{1}{\sqrt{1-\rho^2}} \left( \left( \frac{1-\rho^3}{1-\rho^2} \right) \frac{M}{R} \right)^{k-1}$ ,  $k = 1, \dots, 5$ , can be put in the general

form

$$F_k(\rho) = \frac{(2k-3)!!}{(k-1)!} \left[ \frac{a}{b} \sin^{-1} \rho + \frac{(\pm\sqrt{1-\rho})P(\rho)}{d(1+\rho)^l} \right] \left(\frac{M}{R}\right)^{k-1} \quad (15)$$

where  $a$ ,  $b \neq 0$ ,  $d \neq 0$  are integers;  $P = P(\rho)$  a 'complete' polynomial of degree  $2k-3$  in  $\rho$  for  $k > 1$ , and  $l$  a non-negative

rational number  $< k$ . The  $\pm$  sign in the numerator of the second term signifies that the sign of the term depends on  $k$ . By a 'complete' polynomial of degree  $2k-3$  we mean the polynomial contains terms of every degree up to and including  $2k-3$ . All the variables and integer constants are dependent on  $k$  but we have left out this index in the above symbolism to not clutter the appearance of the general form. Equation (15) also satisfies our condition #2 in that it contains the mass  $M$ . Since the factor  $\frac{a}{b}\sin^{-1}\rho$  term is not present when  $k=2$  then  $a=0$  for this index.

Appendix A lists the antiderivatives for  $k = 1$  to  $5$  which exhibit this general form. The expressions for the constants of integration  $C_k$  are also listed. Although each  $F_k(\rho)$  is derived using a series of trigonometric substitutions and identities during the integration process, there does not seem to be any nice recursive relationship among these antiderivatives or some simple dependency on  $k$ . This would allow us to determine  $F_k(\rho)$  or  $C_k$  for any  $k$  in some closed form. Computations involving higher values of  $k$  are best addressed using software tools due to the large number of terms involved since  $P(\rho)$  is a complete polynomial [see endnote 3 for a paper by Rodriguez and Marin addressing light deflection that encounters a similar issue].

Notice that when  $\rho = 0$ , corresponding to  $r = \infty$ ,  $F_k(\rho)$  reduces to  $\frac{(2k-3)!!}{(k-1)!} \left[ \frac{\pm T}{d} \right] \left( \frac{M}{R} \right)^{k-1}$  where  $T$  is the constant term of  $P(\rho)$ . When  $\rho = 1$   $F_k(\rho)$  reduces to  $\frac{(2k-3)!!}{(k-1)!} \left[ \frac{a}{b} \cdot \frac{\pi}{2} \right] \left( \frac{M}{R} \right)^{k-1}$ . These results are useful when analyzing asymptotic behavior and finding the constant of integration of the antiderivatives.

As an example, compute  $F_5(\rho)$  for  $\rho = 0$ . Using the antiderivative from appendix A:

$$F_5(0) = \left( \frac{35}{8} \right) \left[ \frac{99}{8} \sin^{-1} 0 - \frac{(\sqrt{1-0})P(0)}{56(1+0)^{7/2}} \right] \left( \frac{M}{R} \right)^4 = \left( \frac{35}{8} \right) \left[ -\frac{832}{56} \right] \left( \frac{M}{R} \right)^4 = 65 \left( \frac{M}{R} \right)^4 \quad (16)$$

where  $P(\rho) = 14\rho^7 + 56\rho^6 + 217\rho^5 + 364\rho^4 - 820\rho^3 - 2860\rho^2 - 2691\rho - 832$ .  
So  $P(\rho) = -832$ .

For  $\rho = 1$ ,

$$F_5(1) = \left(\frac{35}{8}\right) \left[ \frac{99}{8} \sin^{-1} 1 - \frac{(\sqrt{1-1})P(1)}{56(1+1)^{7/2}} \right] \left(\frac{M}{R}\right)^4 = \left(\frac{35}{8}\right) \left[ \frac{99}{8} \cdot \frac{\pi}{2} \right] \left(\frac{M}{R}\right)^4 = \left(\frac{3465\pi}{128}\right) \left(\frac{M}{R}\right)^4. \quad (17)$$

Now let

$$\theta_n(\rho) = \sum_1^n F_k(\rho) + C_n \quad (18)$$

where  $C_n$  is the resulting constant of integration. As in section B,  $C_n$  can be found by using the boundary condition that the polar angle is  $\pi/2$  radians when  $r = R$  ( $\rho = 1$ ). As  $n$  increases we can see that  $\theta_n(\rho)$  will involve a large number of terms since  $P = P(\rho)$  is a complete polynomial.

Define

$$\theta_\infty(\rho) \equiv \lim_{n \rightarrow \infty} \theta_n(\rho) = \lim_{n \rightarrow \infty} \sum_1^n F_k(\rho) + C_\infty \quad (19)$$

where  $C_\infty = \lim_{n \rightarrow \infty} C_n$  is the resulting constant of integration in the limit.  $\theta_\infty(\rho)$  is the 'true' theoretical path of the light ray (null geodesic) based on General Relativity. However, truncating  $\theta_\infty(\rho)$  for a sufficiently high cutoff index  $K'$  gives a polar angle to some approximation. In the literature,  $K'$  is traditionally set to a value of 2 when using the antiderivatives to determine the deflection angle for a solar mass.

Using the same boundary conditions as we did with  $\theta_2(\rho)$  and  $\theta_3(\rho)$ , the constant of integration for the light path described by the first five antiderivatives,  $n = 5$ , is determined:

$$\theta_5(1) = \sum_1^5 F_k(1) + C_5 \text{ so } C_5 = \theta_5(1) - \sum_1^5 F_k(1) = \pi/2 - \left\{ \sum_1^5 \frac{(2k-3)!!}{(k-1)!} \left[ \frac{a}{b} \cdot \frac{\pi}{2} \right] \left(\frac{M}{R}\right)^{k-1} \right\} \quad (20)$$

where the  $a$  and  $b$  coefficients depend on  $k$ .

Then

$$\begin{aligned}
 C_5 &= \pi/2 - \left\{ \frac{\pi}{2} + 1 \cdot 0 \frac{\pi}{2} \frac{m}{r_0} + \frac{15\pi}{8} \left(\frac{M}{R}\right)^2 + \frac{5}{2} \left[-3 \frac{\pi}{2}\right] \left(\frac{M}{R}\right)^3 + \frac{35}{8} \left[\frac{99}{8} \cdot \frac{\pi}{2}\right] \left(\frac{M}{R}\right)^4 \right\} \\
 &= -\frac{15\pi}{8} \left(\frac{M}{R}\right)^2 + \frac{15\pi}{4} \left(\frac{M}{R}\right)^3 - \frac{3465\pi}{128} \left(\frac{M}{R}\right)^4.
 \end{aligned} \tag{21}$$

Then the resulting polar angle formula,  $\theta_5(\rho)$ , is

$$\theta_5(\rho) = F_1(\rho) + F_2(\rho) + \dots + F_5(\rho) + C_5. \tag{22}$$

Going forward we will call the ratio  $M/R$  the 'mass ratio'.

We now let the mass ratio in  $\theta_5(\rho)$  range over a selected set of values bounded by  $1/3$ . As a reference point, the mass ratio for the sun is  $M/R \approx 2.1 \times 10^{-6}$  when  $R$  is taken to be at the sun's surface.

Before proceeding further, we now change the notation of the various function arguments to include the mass ratio. Thus change each argument  $(\rho)$  to  $(M/R, \rho)$  and since  $C_n$  is not dependent on  $\rho$  express it as  $C_n \left(\frac{M}{R}\right)$ . Then, (22) is now expressed as

$$\theta_5 \left(\frac{M}{R}, \rho\right) = F_1 \left(\frac{M}{R}, \rho\right) + F_2 \left(\frac{M}{R}, \rho\right) + \dots + F_5 \left(\frac{M}{R}, \rho\right) + C_5 \left(\frac{M}{R}\right). \tag{23}$$

And (19) becomes

$$\theta_\infty \left(\frac{M}{R}, \rho\right) \equiv \lim_{n \rightarrow \infty} \theta_n \left(\frac{M}{R}, \rho\right) = \lim_{n \rightarrow \infty} \sum_1^n F_k \left(\frac{M}{R}, \rho\right) + C_\infty \left(\frac{M}{R}\right) \tag{24}$$

We note that in the limit  $M \rightarrow 0$  (GR flat space),  $\theta_n \left(\frac{M}{R}, \rho\right) = \sum_1^n F_k \left(\frac{M}{R}, \rho\right) + C_n \left(\frac{M}{R}\right)$  equals  $\sin^{-1} \rho$  since  $\frac{M}{R}$  approaches zero. In flat space the light ray path is a straight line going through  $r = R$ , as expected.

We have extended these results to include the next set of antiderivatives  $F_6, \dots, F_{10}$  that exhibit the same form as (15). Due to the completeness of the polynomials  $P = P(\rho)$ , the resulting function contains a large number of terms that we do not show

here. Any such numerical investigation would certainly require extensive use of automation/software tools. Appendix A lists the full expressions for  $F_k$  and  $C_k$ ,  $k = 1, \dots, 5$ .

Going forward we will refer to these models of a light path as ' $n < \infty$ ', ' $n = m$ ' where  $n = m$  for some specified integer  $m$ , or for the infinite case, ' $n = \infty$ '. The model represented by (22) is the  $n = 5$  model and (24) is the  $n = \infty$  model. For the  $n = m$  model,  $n$  will also be referred to as the 'approximation level'.

Proceeding to a fully illustrated example, set  $\rho = 0.95$  (close to the turning point  $R$ ) and  $M/R = 0.1$ . Then a programmed numerical calculation for  $\theta_5$  gives  $\theta_5(M/R = 0.1, \rho = 0.95) = 1.19216$  radians =  $68.3059^\circ$ . The radial distance is found using  $\rho = 0.95$  since  $\rho = R/r = 0.95$  implies  $r = (1/0.95)R = 1.05623R \equiv r_\theta$ . We can also express this as a multiple of the Schwarzschild radius  $\alpha$  by noting that  $\alpha = 2M$  so  $M/R = 0.5\alpha/R = 0.1$  implies  $R = 5\alpha$ . Therefore  $r_\theta = 1.05623(5\alpha) = 5.28115\alpha$ .

Therefore, a member of the light path trajectory for the mass ratio 0.1 at a distance corresponding to  $\rho = 0.95$  is the ordered pair  $(68.3059^\circ, r_\theta = 1.05623R = 5.28115\alpha)$  where all values are to the approximation level  $n = 5$ .

Suppose we let  $M = 1480$  meters which is approximately of solar mass in gravitational units. Then  $R = M/0.1 = 14800$  meters, the turning point of the light path, which is much smaller than the actual radius of our sun. This is of no concern since we have, in most instances, assumed that the mass is point-like. For our chosen value of  $M$ ,  $\alpha = 2M = 2960$  meters. Then the light path member is  $(68.3059^\circ, r_\theta = 1.05623R = 5.28115\alpha = 15632.2 \text{ meters})$ .

If we set  $\rho = 0$  (radial infinity) then  $\theta_5(M/R = 0.1, \rho = 0) = -0.24942$  radians =  $-14.2931^\circ$ . This is the angular value of the asymptotic line through the origin for the path originating at a far distance from the central body that has a turning point at  $R = 14800$ . We will call this line the 'angular asymptotic line'. It can also be viewed as the limiting angle of the radial line if the light ray originated at  $R$  and moved out to infinity.

Computing  $\theta_5$  for all values of  $\rho$  with the above  $M$  and  $R$  generates the entire upper branch of the light path as shown in Fig.2. A symmetry argument yields the lower branch. Since  $n = 5 < \infty$  we know that this only an approximation of the true path represented by  $\theta_\infty(M/R = 0.1, \rho)$ .

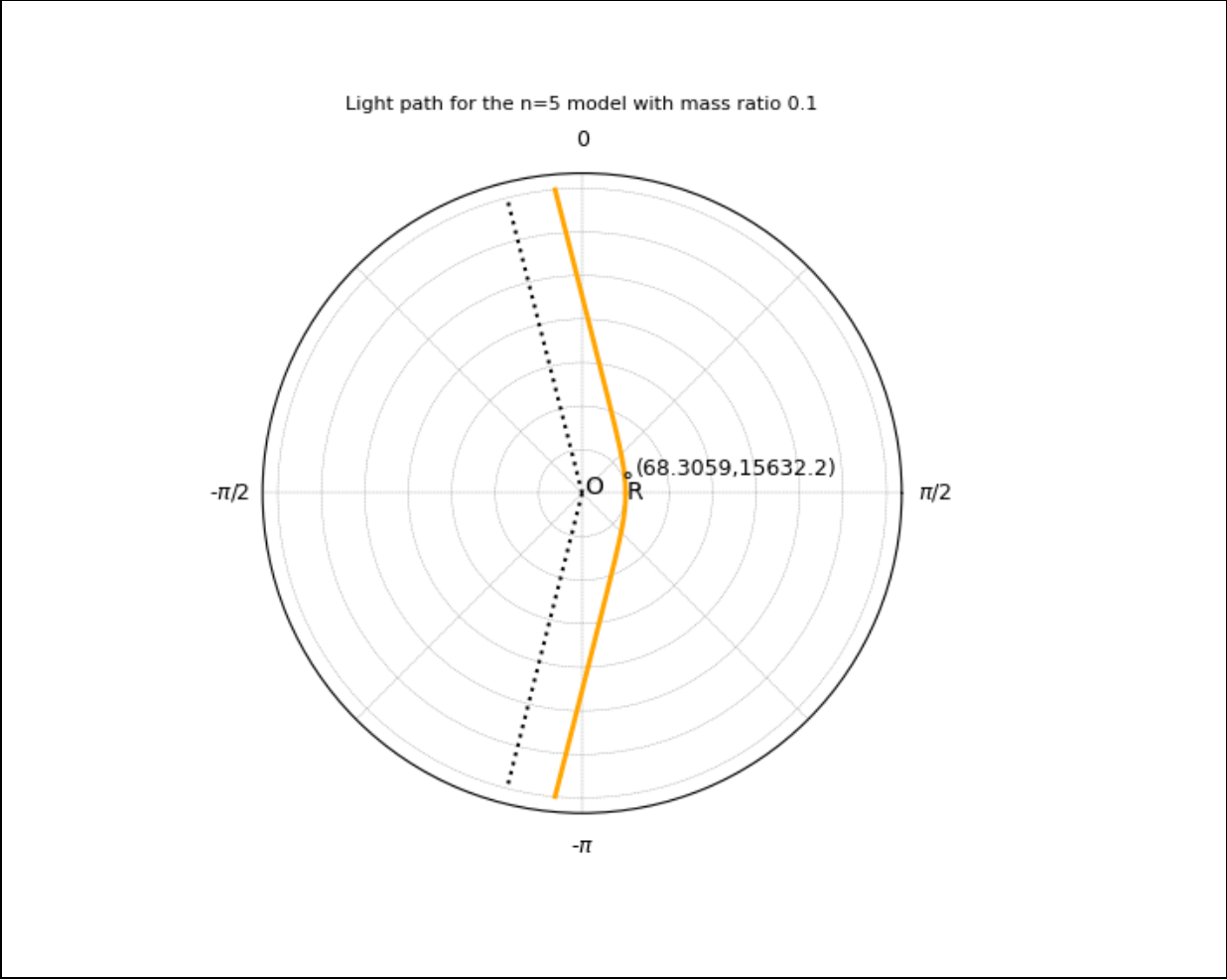


Figure 2. Curved light path for the  $n = 5$  model with mass ratio 0.1, with dotted angular asymptotic lines. The location of the computed light path member  $(\theta, r_\theta) = (68.3059^\circ, 15632.2 \text{ meters})$  is marked. Each radial unit on this graph equals five Schwarzschild radii, the distance of the turning point  $R$  from the center of the mass at the origin  $O$ .

The reader is now referred to Fig.3 that displays an arbitrary light path diagram and the relevant angles and parameters that will be used going forward.

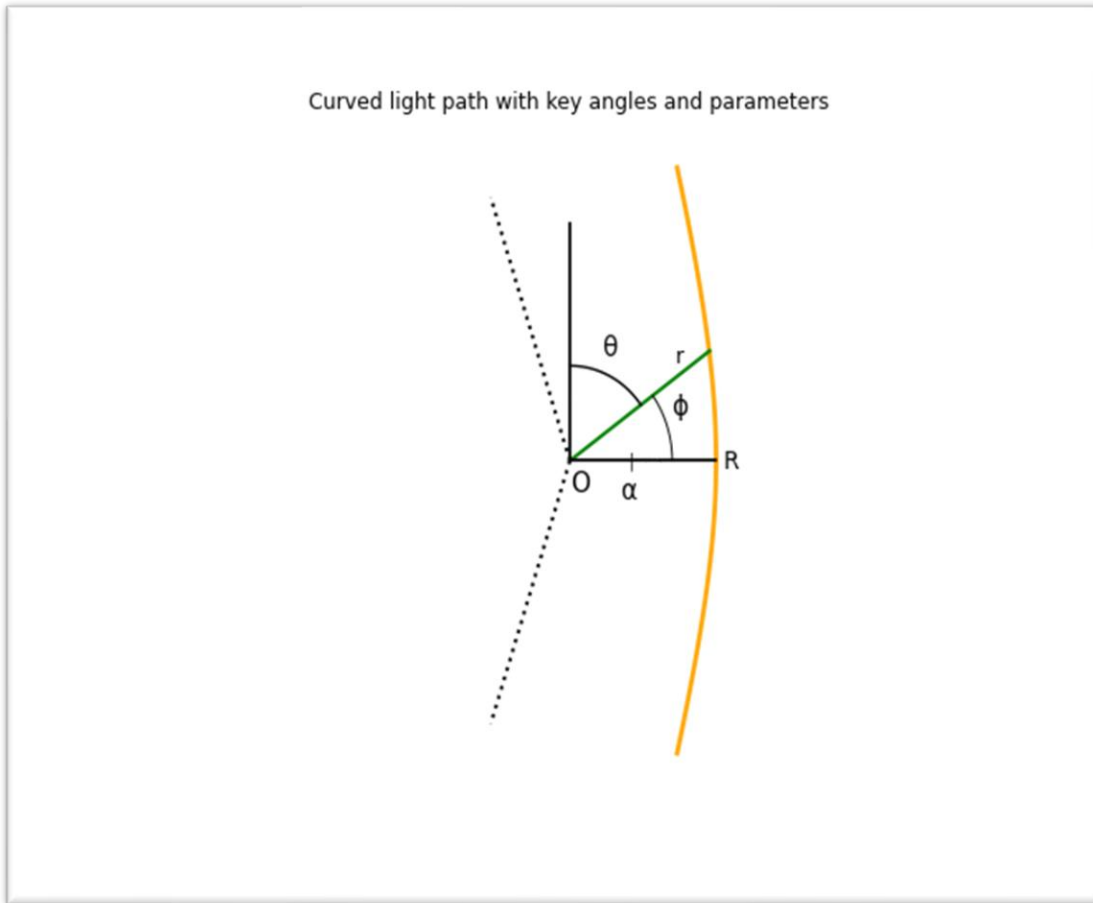


Figure 3. Arbitrary curved light path showing the key angles and parameters going forward. For a light path location in the first quadrant shown,  $\theta$  is the polar angle in spherical coordinates and  $\phi$  the complimentary angle ('vertex' angle) in polar coordinates for the light path location with radial distance  $r$ . The center of the gravitating mass is located at the origin  $O$  with Schwarzschild radius  $\alpha$ . The inbound light path from the angular asymptotic line (upper dotted) passes through the turning point  $R$ , and continues outbound to radial infinity approaching the angular asymptotic line (lower dotted line).

D. Light path equation based on Jacobian elliptic functions:

We now turn to the derived light path equation as expressed in equation (80) of Section 7 in [5], where crucially the equation is in closed form. Going forward we will refer to this light

path model as the HK (Hioe-Kuebel) model. Using the author's original notation:

$$\frac{1}{q} = \frac{(e_1 - e_3)e_2 - (e_2 - e_3)e_1 \operatorname{sn}^2(\gamma\phi, k)}{(e_1 - e_3) - (e_2 - e_3) \operatorname{sn}^2(\gamma\phi, k)}, \quad (26)$$

where the  $e_i$  are roots of a certain cubic in a differential equation expressing how the radial distance  $r$  changes as the angle  $\phi$  varies. This angle is the polar angle in polar coordinates. To avoid confusion with our polar angle  $\theta$  in spherical coordinates we will designate  $\phi$  as the 'vertex' angle going forward. The  $e_i$  roots are in turn functions of  $\alpha/R$  where  $\alpha$  is the Schwarzschild radius of the central body and  $1/q \equiv \alpha/r$  as defined in the HK model. This is all developed in a polar coordinate system with the central body at the origin.

It is not readily apparent, but this HK model and the  $n = \infty$  model are equivalent. Heuristically this can be seen by noting that both models are derived from the same Schwarzschild metric and the GR geodesic equation. A more formal mathematical proof is supplied in appendix B.

The arguments of the Jacobian elliptic function  $\operatorname{sn}$  are  $\gamma\phi$ , the 'amplitude', and  $k$  the 'modulus', where  $\gamma$  and  $k$  are functions of the roots  $e_i$ . Jacobian elliptic functions are a generalization of trigonometric functions which refer to conic sections, the ellipse in particular. For an explanation of these non-elementary functions, including  $\operatorname{sn}$ , see [1], as well as other online sources such as Wikipedia for an introduction.

The roots  $e_i$  take the following values where  $U_1 \equiv \alpha/R$ .

$$\begin{aligned} e_1 &= (1/2) \left[ 1 - U_1 + \sqrt{(1 + 2U_1 - 3U_1^2)} \right] \\ e_2 &= U_1 \\ e_3 &= (1/2) \left[ 1 - U_1 - \sqrt{(1 + 2U_1 - 3U_1^2)} \right] \end{aligned} \quad (27)$$

Also,

$$\gamma = \sqrt{e_1 - e_3}/2 \quad \text{and} \quad k = \sqrt{(e_2 - e_3)/(e_1 - e_3)}. \quad (28)$$

By the Schwarzschild metric  $\alpha = 2M$  and so  $U_1 = \alpha/R = 2M/R$  or  $(1/2)U_1 = M/R$ . Then our mass ratio limit  $0 \leq M/R < 1/3$  implies  $0 \leq U_1 < 2/3$ . Throughout the remainder of the paper we will interchangeably use either  $(1/2)U_1$  or  $M/R$  as the mass term in our equations depending on the context.

Let us now replace  $\frac{1}{q} \equiv \frac{\alpha}{r}$  in (26) with the symbol  $Q$ . Since  $Q$  is dependent on  $U_1$  and  $\phi$  we will use the functional notation  $Q = Q(U_1, \phi)$  analogous to the  $\theta_k = \theta_k\left(\frac{M}{R}, \rho\right)$  notation introduced previously.

Then (26) is expressed as

$$Q(U_1, \phi) = \frac{(e_1 - e_3)e_2 - (e_2 - e_3)e_1 \operatorname{sn}^2(\gamma\phi, k)}{(e_1 - e_3) - (e_2 - e_3) \operatorname{sn}^2(\gamma\phi, k)} \quad (29)$$

The HK model (29) is a function of the vertex angle  $\phi$  and  $U_1$  yielding the radial distance. Conversely, the  $n = 5$  and  $n = \infty$  models (22) and (19) are functions of radial distance and  $M/R$ , giving the polar angles  $\theta_5$  and  $\theta_\infty$ . The necessary conversions and transformations to get a consistent framework to prove the equivalency of the two results is given in the proof in Appendix B.

Similar to the  $n = m$  model we can represent the light path constructed from  $Q = Q(U_1, \phi)$ , in the language of mathematical sets, by the set of ordered pairs  $\{\phi, Q(U_1, \phi)\}_\phi$  where the subscript vertex angle  $\phi$  ranges between 0 and a maximum angular value. The value is dependent on  $U_1$  and is required to generate the entire path; this will be discussed in what follows. Using this viewpoint, we can state that  $\{(\theta_n(M/R, \rho), \rho)\}_\rho = \{\phi, Q(U_1, \phi)\}_\phi$  when  $n = \infty$ , but is only an approximate equality for smaller radial distances when  $n < \infty$  in the sense that that some subset of the ordered pairs are close in value over some subinterval of  $\rho \in [0, 1]$ .

We will now compute an example of a light path location for the same mass ratio  $M/R = 0.1$  used to compute  $r_\theta$  in the example in Section C. Use the angle  $\theta_5 = 68.3059^\circ$  predicted by  $\theta_5(M/R = 0.1, \rho = 0.95)$  as input to  $Q(U_1, \phi)$  to determine if we can recover a radial value  $\approx 5.28115\alpha$ . We first convert  $\theta_5$  to the corresponding complimentary vertex angle which is  $\phi = 90^\circ - 68.3059^\circ = 21.6941^\circ = 0.378633$  radians. This value is now an acceptable input to (29).

Let the radial value we are going to compute be denoted by  $r_\phi$ . Since  $Q(U_1, \phi) = 1/q = \alpha/r_\phi$  then  $r_\phi = \alpha/Q(U_1, \phi)$ . If the two models describe the same light path, given that  $\theta_5$  is an approximation, then we should expect  $r_\phi \approx r_\theta$ .

Computing the values in (27) and (28) to compute  $Q$  we obtain

$$\begin{aligned} e_1 &= 0.965685 \\ e_2 &= 0.2 \\ e_3 &= -0.165685 \\ \gamma &= 0.531830 \\ k &= 0.568527 \end{aligned}$$

where  $U_1 = \alpha/R = \alpha/5\alpha = 0.2$  using  $R = 5\alpha$  which was determined when calculating  $\theta_5$  in the previous section. This  $U_1$  value corresponds to  $M/R = 0.1$ .

We use a Python language routine to compute the  $sn(\gamma\phi, k)$  function. Since the actual computational formula involves an integral that uses the square of the  $k$  argument (see [1]) we will replace  $k$  by  $m = k^2$ . Then  $sn(\gamma\phi, m) = sn(0.531820 \cdot 0.378633, 0.568527^2) = 0.199583$ . Using (29) we have  $Q(U_1 = 0.2, \phi = 0.378633) = 0.190013$ . So  $r_\phi = \alpha/Q = \alpha/0.190013 = 5.2628\alpha$ . In meters this is  $5.2628\alpha = 5.2628(2M) = 5.2628(2960) = 15577.9$ . So  $r_\theta = 5.28115\alpha \approx r_\phi = 5.2628\alpha$  as expected.

If we set  $Q(U_1 = 0.2, \phi) = 0$ , corresponding to radial infinity, then by setting the numerator in (29) equal to zero we can find the vertex angle  $\phi_\infty$  solution for the asymptotic line of the light path. Solving using the inverse elliptic function  $sn^{-1}$  (see [1])

we get  $\phi_\infty = 1.821021$  radians =  $104.337^\circ$ . The corresponding value for the  $n = 5$  model previously computed is  $-14.2931^\circ$  or  $104.2931^\circ$  after converting it to a vertex angle, which closely approximates the HK model.

Computing  $Q(U_1 = 0.2, \phi)$  over a range of  $\phi$  values generates the entire upper branch of the light path as shown in Fig.4. A symmetry argument yields the lower branch. Unlike for the graph of  $\theta_5$  for the  $n = 5$  model in Fig. 2, this is the 'true' path since it is not based on any approximation other than the precision level of the computed constants and variables. Also, unlike the plotting of a light path for a  $n = k$  model, the plotting of a graph for the HK model using (29) can generate 'non-physical' light paths due to the  $sn$  function if the range of  $\phi$  is made too large. In our example we need to restrict this range using the  $\phi$  value found when solving  $Q(U_1 = 0.2, \phi) = 0$ . It is found that the radial values obtained for  $\phi > 104.337^\circ$  (location of the angular asymptote line) do not correspond to an actual light path and should be discarded.

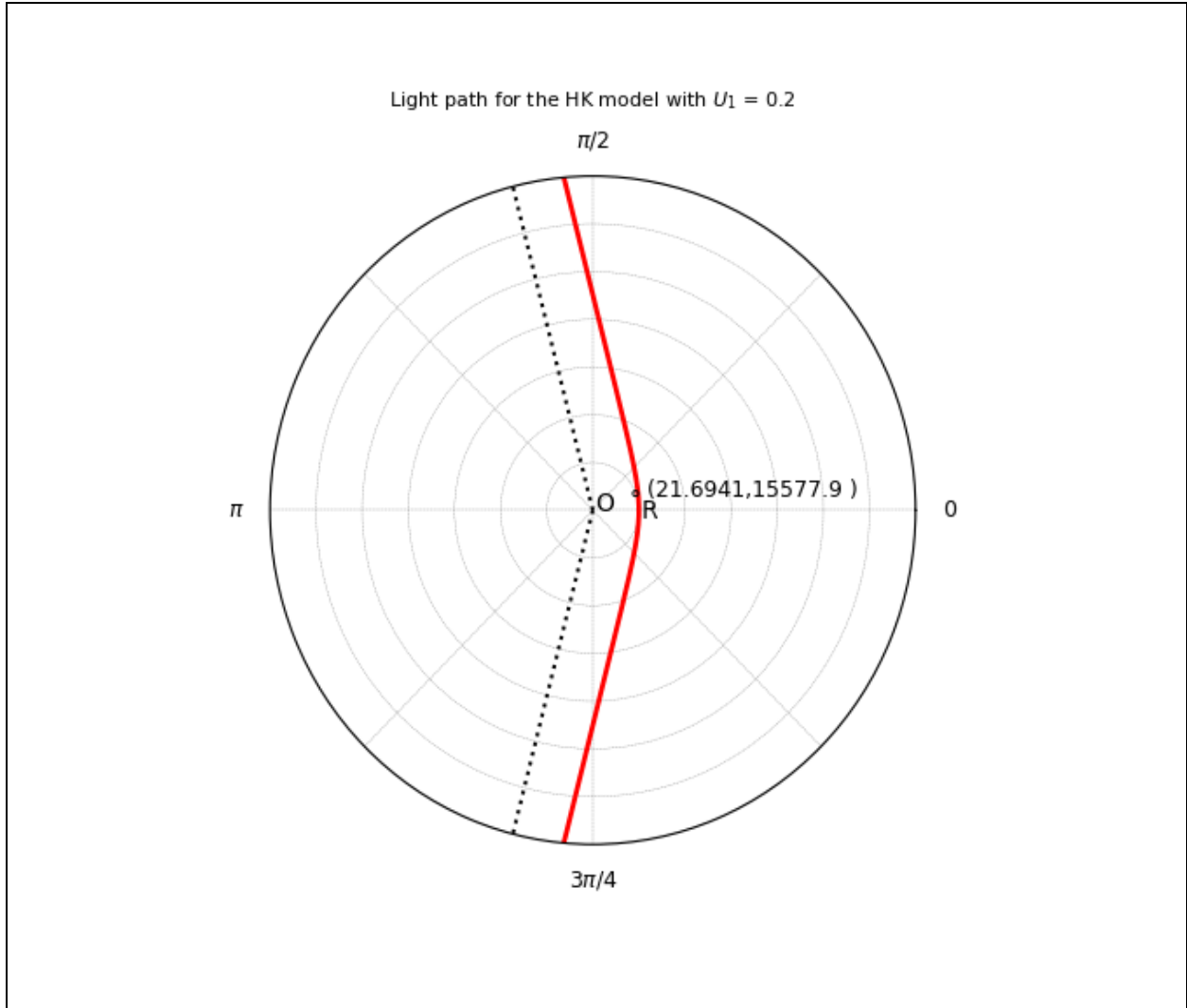


Figure 4. Curved light path in the HK model for  $U_1 = 0.2$  with dotted angular asymptotic lines. The location of the computed light path member  $(\phi, r_\phi) = (21.6941^\circ, 15577.9 \text{ meters})$  is marked. Each radial unit on this graph equals five Schwarzschild radii, the distance of the turning point  $R$  from the center of the mass at the origin  $O$ . Note that the angle labels are for a polar coordinate system as opposed to a spherical coordinate system in Fig. 2 for the  $n = 5$  model.

E. Comparison of the two models:

In the previous section we showed that for  $U_1 = 0.2$  or  $M/R = 0.1$  the  $n = 5$  model appears to closely approximate the HK model based on two methods: 1) a comparison of the predicted HK radial value

for a selected distance from the turning point  $R$  for the  $n = 5$  model, and 2) comparing the angular asymptotic lines. These methods are based on specific radial values, not over the entire range of possible radial values,  $[R, \infty)$ .

It would be nice to have a global quantitative measure to ascertain the 'predictive strength' of an  $n < \infty$  model. Plotting the difference in predicted radial values over the entire range  $[R, \infty)$  is a possibility. A more convenient method is to simply compare the predicted total deflection of each model, which is potentially an observable and, in fact, an actuality for our sun, see [4].

For the  $n < \infty$  model, and suppressing the mass ratio argument, the total deflection  $D_n$  is

$$D_n = 2 [\theta_n(\rho = 0) - \theta_n(\rho = 1)] - \pi.$$

Since  $\theta_n(\rho = 1) = 0$  for all  $M/R$  the above reduces to

$$D_n = 2 [\theta_n(\rho = 0)] - \pi \tag{30}$$

where the polar angle  $\theta_n(\rho = 0)$  is expressed as a vertex angle to compare it to the HK result below.

This formula is derived from the deflection formula in [8] section C.2, step E, equation 5 which is to first order in  $M/R$ . Alternatively, it can be obtained from the work done in section 6.3 of [9]. In either case, we have extended the work to include the higher powers of  $M/R$  present in the Taylor series.

We can see from (30) that it contains the expression for determining the angular asymptotic line, so we are indirectly using this line to help measure the accuracy of the  $n < \infty$  model.

For the HK model, using the deflection formula in [5], equation (82), is

$$D_{HK} = 2 \left[ \frac{2}{\gamma} \operatorname{sn}^{-1}(\psi, m) \right] - \pi, \tag{31}$$

where  $\psi = \left[ \frac{(e_1 - e_3)e_2}{(e_2 - e_3)e_1} \right]^{1/2}$ . The meaning of the variables and the argument convention are described in section D.

Then the global measure of the predictive strength of the  $n < \infty$  model is simply defined as  $P_n(U_1) \equiv [D_n(U_1) - D_{HK}(U_1)]/D_{HK}(U_1)$ . For the  $n = 5$  model the table below gives the predictive strength for selected  $U_1$  values based on total deflection. If  $P_n(U_1) < 0$  then the  $n < \infty$  model underestimates the deflection and for  $> 0$  it overestimates. Values closer to zero indicate more predictive strength. Then for the  $n = \infty$  model,  $P_n(U_1) = 0$ .

$U_1$	$D_n$	$D_{HK}$	$P_n$	Comment
$4.2 \times 10^{-6}$	1.73263 arc seconds	1.80463 arc Seconds	$-3.9898 \times 10^{-2}$	Example: Sun with turning point R at surface
$4.2 \times 10^{-3}$	0.4832260	0.483258	$+3.89043 \times 10^{-6}$	
0.01	1.15718°	1.15722°	$-2.85225 \times 10^{-5}$	
0.1	12.7105°	12.7125°	$-1.52 \times 10^{-4}$	
0.2	28.5862°	28.6614°	$-2.623 \times 10^{-3}$	
0.42922	84.2775°	89.9980°	$-6.3563 \times 10^{-2}$	Deflection = 90° case
0.5	109.444°	125.140°	-0.125425	
0.62470	179.243°	359.996°	-0.502093	Deflection =360° case
0.66	186.638°	481.953°	-0.612746	

Table 1. Selected predictive strength  $P_n$  values for the  $n = 5$  model. Smaller  $U_1$  values have high predictive strength compared to higher  $U_1$  values.  $|P_n|$  values rapidly increase as  $U_1 \rightarrow 2/3$  indicating significantly diminishing predictive strength.

From another perspective, fix the mass and decrease the distance of the turning point R from the central body which increases the  $U_1$  value. Then the predictive strength of the  $n = 5$  model tends to increase based on table 1 but not in a uniform manner.

If we want a more qualitative method to assess the accuracy of the  $n = k$  model we can simply plot the light paths and angular asymptotes out to a given radial distance from the central body.

The plots of both models for  $M/R = 0.25$  ( $U_1 = 0.5$ ) are displayed on one graph in Fig. 5.

The separation of the two paths increases as one moves outward from the turning point  $R$ . The HK light path also exhibits greater curvature - it 'bends' more toward the origin than the  $n = 5$  path. Hence the  $n = 5$  model understates the influence of the central body due to the finite truncation required for computation. This is consistent with the predictive strength values in table 1.

To increase the predictive strength, we would need to use an  $n = k > 5$  model. Such a model possesses more  $F_k$  terms in its formula than for  $n = 5$  so we would expect more accuracy. For much smaller mass ratios such as for the sun where  $M/R \approx 2.1 \times 10^{-6}$  or  $U_1 \approx 4.2 \times 10^{-6}$  (see table 1), the paths and asymptotic lines would be nearly coincident near the central body due to a much smaller gravitational effect.

We do not present the light path based on the Newtonian gravity model but as expected the actual calculated path shows less curvature than either of these models. This is consistent with various experimental observations, starting in 1919 [3,4], of a very small predicted relativistic deflection of  $\approx 1.8$  arc-seconds which is approximately twice that of the Newtonian based prediction. This was first calculated by Johann Soldner early in the 19th century and was also derived independently by Henry Cavendish but in a less than complete manner. See [8] for a detailed analysis.

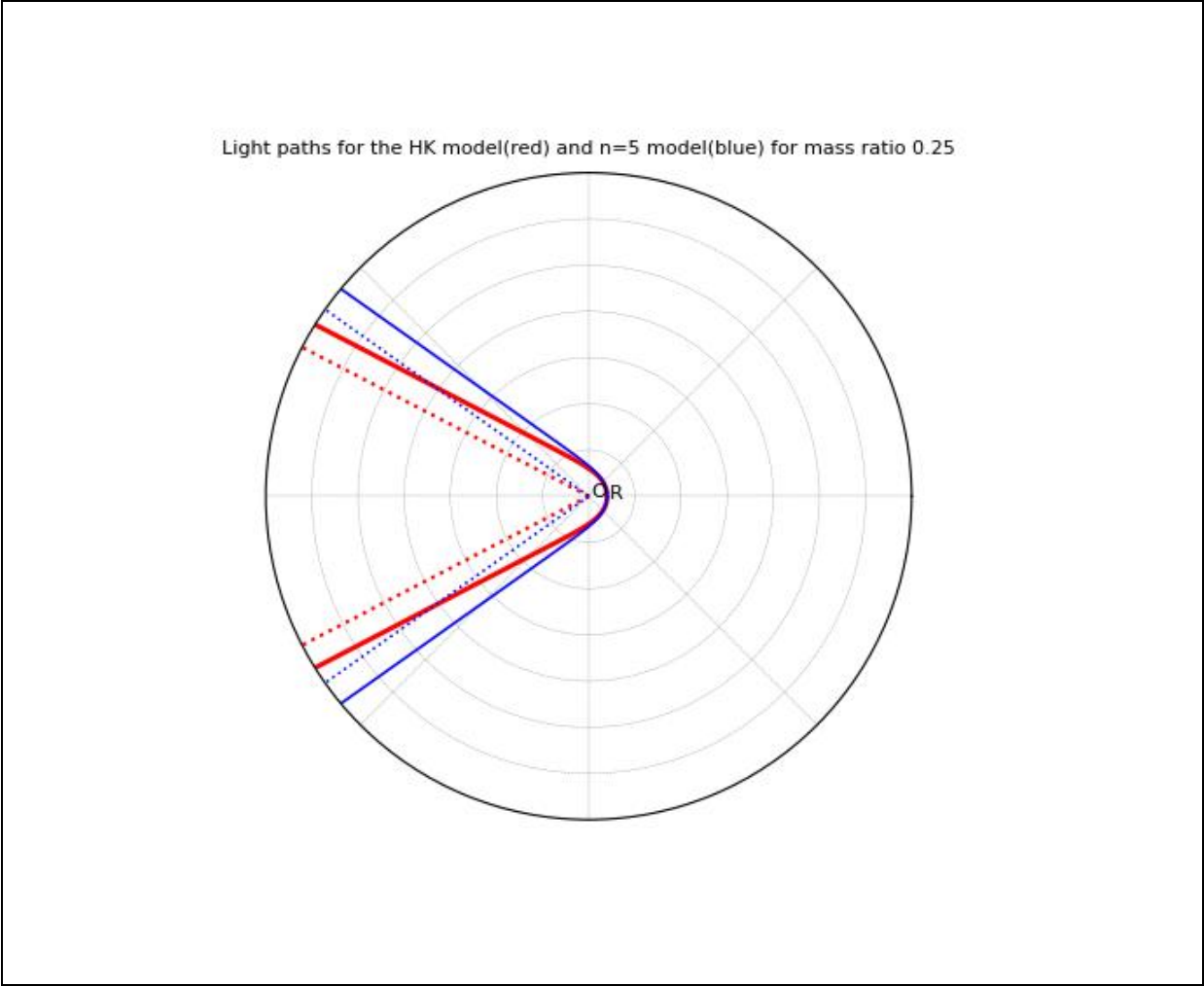


Figure 5. Comparison of light paths with dotted angular asymptotic lines for the HK model (red) and  $n = 5$  model (orange), for mass ratio 0.25. The light paths are clearly diverging as the radial value increases out to 35 Schwarzschild radii. Each radial unit on this graph equals 5 Schwarzschild radii, the distance of the turning point  $R$  from the center of the mass at the origin  $O$ .

Summary:

We first derived the light path equation

$$\theta_{\infty} \left( \frac{M}{R}, \rho \right) \equiv \lim_{n \rightarrow \infty} \theta_n \left( \frac{M}{R}, \rho \right) = \lim_{n \rightarrow \infty} \sum_1^n F_k \left( \frac{M}{R}, \rho \right) + C_{\infty} \left( \frac{M}{R} \right)$$

for the  $n = \infty$  model and its finite companion  $n = 5$  model

$$\theta_5 \left( \frac{M}{R}, \rho \right) = F_1 \left( \frac{M}{R}, \rho \right) + F_2 \left( \frac{M}{R}, \rho \right) + \dots + F_5 \left( \frac{M}{R}, \rho \right) + C_5 \left( \frac{M}{R} \right).$$

These equations were derived using a Taylor series expansion of functions derived from the Schwarzschild metric and GR geodesic equation. Each term in the series is built from elementary functions - inverse trigonometric functions, polynomials, and rational powers of polynomials.

Next, a light path equation in closed form which we call the HK model, as developed in [5], was described:

$$Q(U_1, \phi) = \frac{(e_1 - e_3)e_2 - (e_2 - e_3)e_1 \operatorname{sn}^2(\gamma\phi, k)}{(e_1 - e_3) - (e_2 - e_3) \operatorname{sn}^2(\gamma\phi, k)}.$$

This model uses the Jacobian elliptic function  $\operatorname{sn}$ . We then proved this is equivalent to  $\theta_\infty\left(\frac{M}{R}, \rho\right)$  for the mass ratio  $M/R < 1/3$ .

Quantitative and graphical comparisons of the HK model with the  $n=5$  model were then given where we introduced the predictive strength measure  $P_n$ . As  $U_1$  increases, the predictive strength apparently decreases but we do not prove it in this paper.

#### Endnotes:

1. The metric can be represented by the proper time line element  $d\tau^2 = \left(1 - \frac{2m}{r}\right) dt^2 - \left(1 - \frac{2m}{r}\right)^{-1} dr^2 - r^2 d\theta^2 - r^2 (\sin\theta)^2 d\phi^2$  which contains the gravitational tensor components. This characterizes the curvature of space-time around a spherically symmetric body in a vacuum and is a solution of the Einstein Field Equation for that physical system.
2. In GR, mass is frequently converted to units of length in meters ('gravitational units') using the conversion factor  $G/c^2$ .
3. A similar pattern of fractional values of pi is found in C. Rodriguez, and C. Marin, "Higher-order corrections for the deflection of light around a massive object". ArXiv:1704.04434. (2017). Refer to Table I. The origin of

these patterns is the tensor components of the Schwarzschild metric.

Appendix A: List of antiderivatives  $F_k$  and constants of integration  $C_n$ .

Antiderivatives:

$$F_1 = \sin^{-1} \rho$$

$$F_2 = -\frac{(\sqrt{1-\rho})(\rho+2)}{(1+\rho)^{1/2}} \left(\frac{M}{R}\right)$$

$$F_3 = \left(\frac{3}{2}\right) \left[ \frac{5}{2} \sin^{-1} \rho - \frac{(\sqrt{1-\rho})(3\rho^3+6\rho^2-7\rho-8)}{6(\rho+1)^{3/2}} \right] \left(\frac{M}{R}\right)^2$$

$$F_4 = \left(\frac{5}{2}\right) \left[ -3\sin^{-1} \rho - \frac{(\sqrt{1-\rho})(5\rho^5+15\rho^4+70\rho^3+247\rho^2+306\rho+122)}{15(1+\rho)^{5/2}} \right] \left(\frac{M}{R}\right)^3$$

$$F_5 = \left(\frac{35}{8}\right) \left[ \frac{99}{8} \sin^{-1} \rho - \frac{(\sqrt{1-\rho})(14\rho^7+56\rho^6+217\rho^5+364\rho^4-820\rho^3-2860\rho^2-2691\rho-832)}{56(1+\rho)^{7/2}} \right] \left(\frac{M}{R}\right)^4$$

The above  $F_k$ , and  $F_6$  through  $F_{10}$  (not shown), are of the form  $\frac{(2k-3)!!}{(k-1)!} \left[ \frac{a}{b} \sin^{-1} \rho + \frac{(\pm\sqrt{1-\rho})P(\rho)}{d(1+\rho)^l} \right] \left(\frac{M}{R}\right)^{k-1}$  as defined in section C.

Constants of Integration:

$$C_1 = 0$$

$$C_2 = 0$$

$$C_3 = C_2 - \frac{15\pi}{8} \left(\frac{M}{R}\right)^2$$

$$C_4 = C_3 + \frac{15\pi}{4} \left(\frac{M}{R}\right)^3$$

$$C_5 = C_4 - \frac{3465\pi}{128} \left(\frac{M}{R}\right)^4$$

$$C_n = C_{n-1} - F_n(\rho = 1) \text{ where for } n = 1, 2, \dots, 10,$$

$$F_n(\rho = 1) = \frac{(2n-3)!!}{(n-1)!} \left[ \frac{a}{b} \cdot \frac{\pi}{2} \right] \left(\frac{M}{R}\right)^{n-1} \text{ for integers } a, b \text{ that depend on } n.$$

Appendix B: Proof of the equivalence of the two light path models  $n = \infty$  and HK.

We will not directly transform the  $n = \infty$  model equation (24) to the HK equation (26). Instead, we will show that (3)

$$d\theta = \frac{d\rho}{\sqrt{\left[1 - \rho^2 - \frac{2M}{R}(1 - \rho^3)\right]}}, \quad (\text{B.1})$$

which is derived from the GR geodesic equation applied to the Schwarzschild metric and which leads to (24), can be transformed to the equation

$$\left(\frac{dU}{d\phi}\right)^2 = (e_1 - U)(e_2 - U)(U - e_3). \quad (\text{B.2})$$

Where  $U \equiv \alpha/r$ , and the constants  $e_i$  have been previously defined in section D. This equation is also derived from the same Schwarzschild metric. The authors then show that (B.2) yields (26). Thus (24) and (26) should be equivalent since no additional differing physical assumptions are introduced in the author's derivations in this paper and [5].

We now proceed to demonstrate the equivalence. As cautioned in the Introduction, the key equations here are drawn from several sources, each with their own notation and conventions. This will necessitate performing multiple sets of transformations which, although being somewhat tedious, will be necessary to demonstrate our assertion of equivalence.

Proceeding with the proof and starting with (B.1) a series of algebraic steps are applied:

$$d\theta = \frac{d\rho}{\sqrt{\left[1 - \rho^2 - \frac{2M}{R}(1 - \rho^3)\right]}} = \frac{d\rho}{\sqrt{\left[\frac{2M}{R}\rho^3 - \rho^2 + 1 - \frac{2M}{R}\right]}} = \frac{d\rho}{\sqrt{\frac{2M}{R}\left[\rho^3 - \left(\frac{2M}{R}\right)^{-1}\rho^2 + \left(\frac{2M}{R}\right)^{-1}\left(1 - \frac{2M}{R}\right)\right]}}. \quad (\text{B.3})$$

We have previously shown in Section B that the radicand is greater than zero in all cases, avoiding any possibility of complex numbers.

Define  $G \equiv \left(\frac{2M}{R}\right)^{-1}$ . Then the radicand of the denominator in (B.3) becomes

$G^{-1}[\rho^3 - G\rho^2 + G(1 - G^{-1})]$ . Note that  $\rho = 1$  is a root of the bracketed cubic equation. Then we have  $G^{-1}(\rho - 1)$ (some quadratic) and therefore

$$G^{-1}[\rho^3 - G\rho^2 + G(1 - G^{-1})] = G^{-1}(\rho - 1)(\text{some quadratic}). \quad (\text{B.4})$$

Using synthetic division by dividing  $(\rho - 1)$  into  $[\rho^3 - G\rho^2 + G(1 - G^{-1})]$  we arrive at

$$G^{-1}[\rho^3 - G\rho^2 + G(1 - G^{-1})] = G^{-1}(\rho - 1)(\rho^2 + \rho(1 - G) + 1 - G). \quad \text{So now} \\ (\text{B.3}) \text{ is written as}$$

$$d\theta = \frac{d\rho}{\sqrt{G^{-1}(\rho-1)(\rho^2+\rho(1-G)+1-G)}}. \quad (\text{B.5})$$

Factoring the quadratic in  $\rho$  we get

$$d\theta = \frac{d\rho}{\sqrt{G^{-1}(\rho-f_2)(\rho-f_1)(\rho-f_3)}} \quad (\text{B.6})$$

where  $f_2 = 1$ ,

$$f_1 = \frac{1}{2} \left[ -(1 - G) + \sqrt{(1 - G)^2 - 4(1 - G)} \right] = \frac{1}{2} \left[ (G - 1) + \sqrt{G^2 + 2G - 3} \right], \text{ and} \\ f_3 = \frac{1}{2} \left[ -(1 - G) - \sqrt{(1 - G)^2 - 4(1 - G)} \right] = \frac{1}{2} \left[ (G - 1) - \sqrt{G^2 + 2G - 3} \right].$$

Now rewrite (B.6) as

$$\frac{d\theta}{d\rho} = \frac{1}{\sqrt{G^{-1}(\rho-f_2)(\rho-f_1)(\rho-f_3)}}. \quad (\text{B.7})$$

Transforming this equation to the variables and notation used in the HK model and defining some new variables and constants:

- a)  $G^{-1} = \frac{1}{G} = \frac{1}{\left(\frac{2M}{R}\right)^{-1}} = \frac{2M}{R} = \frac{\alpha}{R} \equiv U_1$ , where  $\alpha = 2M$  is the Schwarzschild radius,
- b)  $U \equiv \frac{\alpha}{r}$ ,
- c)  $\rho = \frac{R}{r} = R \frac{1}{r} = R \frac{U}{\alpha} = \frac{R}{\alpha} U = U_1^{-1} U$ .

Our goal now is to transform (B.7) into an equation in terms of  $U_1$ . The authors employ this key parameter since it contains the point of closet approach  $R$ , analogous to our  $n = k$  model which employs  $\rho$  which also contains  $R$ .

Then rewrite  $f_1, f_3$  as

$$f_1, f_3 = \frac{1}{2} \left[ (U_1^{-1} - 1) \pm \sqrt{(U_1^{-1})^2 + 2U_1^{-1} - 3} \right] = \frac{1}{2} \left[ \frac{1 - U_1 \pm \sqrt{1 + 2U_1 - 3U_1^2}}{U_1} \right], \quad (\text{B.8})$$

and as before  $f_2 = 1$ .

Next, from the above

$$d\rho = d(U_1^{-1}U) = U_1^{-1}dU = U_1^{-1}d\frac{\alpha}{r} = U_1^{-1}\alpha\left(-\frac{1}{r^2}\right)dr = -U_1^{-1}\frac{\alpha}{r}dr = -U_1^{-1}U\frac{1}{r}dr.$$

Then (B.7) can be expressed as

$$\frac{d\theta}{-U_1^{-1}U\frac{1}{r}dr} = \frac{1}{\sqrt{U_1(U_1^{-1}U-1)(U_1^{-1}U-f_1)(U_1^{-1}U-f_3)}}. \quad (\text{B.9})$$

Simplifying further

$$\frac{d\theta}{dr} = \frac{-U_1^{-1}U}{r\sqrt{U_1(U_1^{-1}U-1)(U_1^{-1}U-f_1)(U_1^{-1}U-f_3)}}. \quad (\text{B.10})$$

Then applying (B.8) and some algebra, the cubic in the radicand is changed to

$$U_1(U_1^{-1}U-1)\left(U_1^{-1}U-\frac{1}{2}\left[\frac{1-U_1+\sqrt{1+2U_1-3U_1^2}}{U_1}\right]\right)\left(U_1^{-1}U-\frac{1}{2}\left[\frac{1-U_1-\sqrt{1+2U_1-3U_1^2}}{U_1}\right]\right). \quad (\text{B.11})$$

More algebra gives

$$U_1^{-2}(U-U_1)\left(U-\frac{1}{2}\left[1-U_1+\sqrt{1+2U_1-3U_1^2}\right]\right)\left(U-\frac{1}{2}\left[1-U_1-\sqrt{1+2U_1-3U_1^2}\right]\right). \quad (\text{B.12})$$

Then (B.10) is written as

$$\frac{d\theta}{dr} = \frac{-U_1^{-1}U}{r\sqrt{U_1^{-2}(U-U_1)\left(U-\frac{1}{2}\left[1-U_1+\sqrt{1+2U_1-3U_1^2}\right]\right)\left(U-\frac{1}{2}\left[1-U_1-\sqrt{1+2U_1-3U_1^2}\right]\right)}} = \frac{-U}{r\sqrt{(U-U_1)\left(U-\frac{1}{2}\left[1-U_1+\sqrt{1+2U_1-3U_1^2}\right]\right)\left(U-\frac{1}{2}\left[1-U_1-\sqrt{1+2U_1-3U_1^2}\right]\right)}}. \quad (\text{B.13})$$

The cubic in  $U$  of the radicand has the roots

$$\begin{aligned} e_2 &\equiv U_1 \\ e_1 &\equiv \frac{1}{2}\left[1-U_1+\sqrt{1+2U_1-3U_1^2}\right] \\ e_3 &\equiv \frac{1}{2}\left[1-U_1-\sqrt{1+2U_1-3U_1^2}\right]. \end{aligned} \quad (\text{B.14})$$

These now match the roots given in (78) of [5]. We only need to do additional manipulations and replace  $\theta$  with  $\phi$ .

Inverting  $\frac{d\theta}{dr}$  and observing that  $dr = d\left(\frac{\alpha}{U}\right) = -\frac{\alpha}{U^2}dU$  we carry out the following algebraic steps:

$$\begin{aligned} \frac{dr}{d\theta} &= -\frac{\alpha}{U^2} \frac{dU}{d\theta} = \frac{r\sqrt{(U-e_2)(U-e_1)(U-e_3)}}{-U} \rightarrow \\ \frac{\alpha}{U} \frac{dU}{d\theta} &= r\sqrt{(U-e_2)(U-e_1)(U-e_3)} \rightarrow \\ \frac{\alpha}{\alpha/r} \frac{dU}{d\theta} &= r\sqrt{(U-e_2)(U-e_1)(U-e_3)} \rightarrow \\ \frac{dU}{d\theta} &= \sqrt{(U-e_2)(U-e_1)(U-e_3)}. \end{aligned} \quad (\text{B.15})$$

To bring  $\phi$  into the equation note that as explained in Fig. 3,  $\theta$  is the polar angle and  $\phi$  is vertex angle. Then they are complimentary, meaning  $\theta + \phi = \pi/2$ , so  $d\theta = -d\phi$ . Then the last equation, (B.15), is now

$$\frac{dU}{d\phi} = -\sqrt{(U-e_2)(U-e_1)(U-e_3)}. \quad (\text{B.16})$$

Reversing the order of the terms in the first two factors preserves the sign and reordering the factors we arrive at

$$\left(\frac{dU}{d\phi}\right)^2 = (e_1 - U)(e_1 - U)(U - e_3). \quad (\text{B.17})$$

This now matches the author's equation (79) in [5]. This is used to obtain their light path equation (80) which we have labeled equation (26) in this paper. Their derivation partly relies on tables of Jacobian Elliptic Integrals. See page 74 of [1], integrand 234.00, for the relevant integral. The integrand requires the ordering  $e_1 > e_2 > U > e_3$  which the author's claim. This can be verified using the formulas for  $e_i$  in (B.14) and  $0 \leq U_1 \leq 2/3$  to compute a solution interval for each root and then comparing the upper and lower values of each interval.

Recall that we started this proof specifying that  $0 < M/R < 1/3$  which corresponds to  $0 < U_1 < 2/3$  since  $U_1 = \alpha/R = 2M/R$ . This range for  $U_1$  places it within 'region I' of the HK model as described in [5].

This completes the proof.

Acknowledgments: I would like to thank Professor Hioe of the University of Rochester and St. John Fisher College(emeritus) for providing valuable insight and a better understanding of the Hioe-Kuebel paper [5] in a series of e-mail communications.

References:

[1] Byrd, Paul F. and Friedman, Morris D., "Handbook of Elliptic Integrals for Engineers and Scientists", 2<sup>nd</sup> edition Revised. Springer-Verlag. (1971)

[2] Carroll, Sean M., "Spacetime and Geometry: An Introduction to General Relativity" 1st Edition. Cambridge University Press. (2019)

[3] Einstein, A., "The Meaning of Relativity". Methuen & Co. Ltd. London, Fourth edition, pp 88-89. (1950). This book is

based on a series of lectures he gave in 1921 at Princeton University and contains his now famous correct deflection prediction based on General Relativity. The original paper containing the prediction was published in 1916 as "Die Grundlage der allgemeinen Relativitätstheorie", *Annalen der Physik*, 49.

[4] Goldoni, Emanuelle and Stefanini, Ledo, "A Century of Light-Bending Measurements: Bringing Solar Eclipses into the Classroom", arXiv:2002.01179v1, (2020). In the context of a learning experience for students, describes several key measurements of light deflection from 1919 through 2017.

[5] Hioe, F.T. and Kuebel, David, "Characterizing Planetary Orbits and the Trajectory of Light", arXiv:1001.0031v1. (2009)

[6] Landau, L.D. and Lifschitz, E.M., "*The Classical Theory of Fields*", section 101, 4rth Revised English Edition, Elsevier. (1975)

[7] Magnan, Christian, "Complete calculations of the perihelion precession of Mercury and the deflection of light by the Sun in General Relativity", arXiv:0712.3709. (2007). The author's demonstration uses only elementary algebra without resorting to tensor formalism.

[8] Malczewski, G. and Selig, D., "A History of Light Deflection with Newtonian and General Relativity Perspectives", VixRa 2304-0099, version 4. (2024)

[9] Wald, Robert M., "*General Relativity*". The University of Chicago Press. (1984)